Journal of Analytical and Applied Pyrolysis 172 (2023) 106008

Contents lists available at ScienceDirect

Journal of Analytical and Applied Pyrolysis

journal homepage: www.elsevier.com/locate/jaap

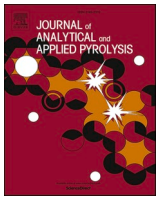

Establishing the origin of aromatic products from vascular and non-vascular vegetation inputs in surficial peats using ^{13}C-labelled tetramethylammonium hydroxide (TMAH) thermochemolysis

Eleanor Y. Reed [a,1], Christopher H. Vane [b], Geoffrey D. Abbott [a,*]

[a] School of Natural & Environmental Sciences, Drummond Building, Newcastle University, Newcastle upon Tyne NE1 7RU, UK
[b] British Geological Survey, Keyworth, Nottingham NG12 5GG, UK

ARTICLE INFO

Keywords:
Sphagnum
Lignin
TMAH
THM
Peat
Vegetation biomarkers

ABSTRACT

Six cambic stagnohumic gley soil profiles located on marginal peatland between a gymnosperm plantation (Sitka spruce (*Picea sitchensis* (Bong.) *Carr.*)) and heather grassland in Wark Forest (northeast England), were analysed using ^{13}C labelled tetramethylammonium hydroxide (TMAH) thermochemolysis to yield methylated phenolic and oxygenated aromatic products. The identification of aromatic compounds derived from the thermally assisted hydrolysis and methylation (THM) of vascular plant, *Sphagnum* and non-*Sphagnum* spp. allowed changes in vegetation both within the top 50 cm of peat (surficial peat) and across the site to be explored. Four sphagnum acid pyrolysis products reflected the presence of *Sphagnum* spp.; lignin phenols reflected the presence of vascular inputs; whilst 3,4-dimethoxybenzenepropanoic acid methyl ester reflected the presence of the non-*Sphagnum* moss *Polytrichum commune*. ^{210}Pb dating of the surficial peat suggests that a historic change in vegetation identified by the changes in aromatic compound distribution with depth, coincide with the adjacent plantation of coniferous woodland. The peat closest to the plantation has seen a shift from grass dominated vegetation, to a species diverse vegetation cover, including *Sphagnum* spp. and vascular vegetation. These results suggest that *Sphagnum* spp. are able to survive not only perturbing environmental conditions, but are also able to establish themselves amongst non-*Sphagnum* species. This study demonstrates the ability of ^{13}C-TMAH THM to be utilised as a screening method for the rapid characterisation of aromatic biomacromolecules in peat to identify key historic and current vegetation inputs. This technique in combination with peat dating helps identify the degradation patterns of these inputs and associated carbon dynamics, providing information on the resilience of current peat deposits to climate change and changing peat conditions.

1. Introduction

The environmental benefits of healthy organic-rich soils are well documented, from their ability to store vast quantities of carbon [1] to their capacity to support rare and diverse flora and fauna [2]. However, between the 1950 s and 1980 s approximately 190,000 ha of deep peats and 315,000 ha of shallow peats in Britain alone were drained, ploughed and planted with coniferous forest [3]. The extensive ground preparation accelerates the oxidation of the stored carbon due to a disturbed soil structure and broken soil aggregates, lowered water table, decreased soil moisture and peat aeration [4–6]. These physical changes can induce changes to the vegetation both within the plantation site and the adjacent land.

Pockets of unplanted peat have remained at many plantation sites due to their unsuitability for timber production [7]. These areas can experience vegetation changes, for example, the vegetation cover of unplanted peat at Wark Forest shifted from a *Sphagnum* dominated vegetation cover in the late 1950 s to a mixed *Eriophorum angustifolium* (cotton grass), *Calluna* (heather) and grass vegetation (e.g. *Festuca ovina, Deschampsia flexuosa* and *Eriophorum vaginatum*) cover in the late 1980 s [8]. Furthermore, the spreading of coniferous, gymnosperm forest species from forest plantations onto areas of open peat has been seen to have a significant negative impact upon the landscape by further reducing the area of natural habitat [9].

* Corresponding author.
E-mail address: geoff.abbott@newcastle.ac.uk (G.D. Abbott).
[1] Present address: Natural England, Lancaster House, Newcastle upon Tyne, NE4 7YH, UK

https://doi.org/10.1016/j.jaap.2023.106008
Received 30 November 2022; Received in revised form 4 May 2023; Accepted 11 May 2023
Available online 12 May 2023

Sphagnum is the dominant peat forming moss and is regarded as extremely recalcitrant due to the high content of sphagnum acid in the cell walls [10,11]. In addition to *Sphagnum* spp., there are also vascular plants associated with peat accumulation which will contribute lignin and other polyphenols to the peat litter, including non-*Sphagnum* mosses (e.g. *Polytrichum commune, Pleurozium schreberi*), *Calluna vulgaris* and grasses (e.g. *Festuca ovina, Deschampsia flexuosa* and *Eriophorum vaginatum*). After cellulose and hemicellulose, lignin is the most abundant biopolymer in vascular species [12,13], and accounts for approximately a third of the organic carbon in the biosphere [14]. The chemical composition and structure of lignin can vary widely between different vascular plant groups, and therefore can provide an excellent vegetation indicator. Lignin can be divided into three main chemotaxonomic groups namely gymnosperm, angiosperm and grass lignin (non-woody) [15].

Vegetation assessments are typically undertaken through time consuming, repeated visual assessment of vegetation quadrats to establish changes over time (e.g. UKCEH Countryside Survey) [16]. However, when historic records of past vegetation are not available, alternative techniques need to be employed. Thermally assisted hydrolysis and methylation (THM) in the presence of ^{13}C-labelled tetramethylammonium hydroxide (TMAH) has been successfully used to analyse a variety of biopolymers, soil organic matter and dissolved organic matter [17–23]. Pyrolysis has been utilised to analyse the lignin biomacromolecule in soils [24]. To aid the structural identification of macromolecules, thermochemolysis in the presence of TMAH was introduced as a pyrolytic degradation technique with in-situ derivatisation [25].

The ^{13}C-labelled TMAH methylates phenolic acids and phenols using ^{13}C-labelled methyl groups. This method distinguishes methoxyl groups pre-existing to TMAH treatment, from those incorporated into hydroxyl phenolic groups in the case of vegetation devoid of lignin, allowing the distinction between lignin, altered lignin and non-lignin phenols. Abbott et al., and Swain & Abbott [26,27] displayed the ability of this technique to identify *Sphagnum* moss biomarkers in peat soils, and identified the use of the relative amounts of the four sphagnum acid THM products as indicators of redox conditions in young surficial peats; whilst Nierop et al., [17] have demonstrated the ability of this method to identify sporomorph-derived sporopollenins, including those from non-*Sphagnum* mosses.

It has been shown that different plant genera [11,28,29], and even different species input [30,31] can have an effect on the degree of degradation in peat [32]. This results in species-specific degrees of degradation, therefore any humification measurements of bulk peat, which can be used as a palaeoclimate proxy can be misleading without accounting for interactions between climate and vegetation and implications for changing peat degradation [32].

^{210}Pb dating has been utilised to calculate chronologies of young peat sequences, typically deposited during the last 150–300 years [33,34]. ^{13}C-TMAH THM coupled with ^{210}Pb dating, is utilised in this paper as a screening method for the rapid characterisation of aromatic biomacromolecules in surficial peat across a macrotopographic gradient within Wark Forest, UK, as a function of depth. Three areas were investigated on marginal peat soils between a Sitka spruce plantation and open heather dominated grassland. The objective was to explore the key aromatic products for specific vegetation and evaluate the changes of the chemical characteristics as a function of depth.

2. Material and methods

2.1. Site description

Wark Forest, a 13.5 km^2 catchment located within the southern part of Kielder Forest, northeast England (55°04'N, 2°18'W, elevation 160–240 m AOD, annual precipitation 1350 mm yr^{-1}) [7]. Wark Forest consists primarily of Sitka spruce, Norway spruce (*Picea abies*), and Lodgepole pine (*Pinus contorta*) established in the 1930 s on moorland and enclosed pastures [8,35]. Small pockets of open peat remain, one of which is the subject of this study, currently mapped as heather grassland [36]. Vegetation observed in Coom Rigg Moss (55°10`N, 2°48`W), a pocket of raised bog peat to the west of the study site has a ground vegetation of heather and grasses (*Calluna vulgaris*, *Deschampsia flexuosa* and *Eriophorum vaginatum*), and has been designated a National Nature Reserve in 1960 [8].

The study area comprises seasonally wet, deep peat to loam soils (cambic stagnohumic gley soil). These soils are typically acidic, slowly permeable, seasonally waterlogged, fine loamy and fine loamy over clayey upland soils with a peaty surface horizon [37]. Drains have been created in the adjacent coniferous plantation to make the typically waterlogged soil more favourable for growing Sitka spruce, by reducing the water table and increasing aeration.

The pocket of unplanted peat of interest in this study displays three distinct areas. The open peat (OP) displays characteristics typical of peatland, including a hummock-hollow topography and a natural vegetation cover. Around 200 m east from this open peat moving towards the plantation, there is an encroachment of Sitka spruce onto the peat which has occurred via self-seeding. This is the forest-peat margin which could be further split into two distinct areas approximately 50 m apart; the forest-margin (FM), an area of peat that has lost the distinctive hummock-hollow topography but remains relatively open, and the Sitka spruce (SS) area, in which the self-seeded Sitka spruce have become established.

2.2. Sample collection and preparation

Two soil profiles were dug at each of the three distinct areas to a depth of 50 cm to represent the surficial peat, with samples taken from each identified soil horizon in March 2010. The soil profiles sampled were entirely organic, with samples taken from the litter and three ectorganic layers; fresh litter (L), fibric histic (Hf), mesic histic (Hm) and the sapric histic (Hs) horizons. The separate horizons were identified through the proportion of visible plant litter fibres and degree of decomposition. Peat degradation displays a continuum from easily identifiable plant remains, through to completely decomposed peat with no discernible plant structure, as described in the Von Post Humification Scale [38]. Horizon depths are shown in Table 1.

Soils were returned to the laboratory within 24 h of collection and stored in the freezer prior to freeze-drying. Prior to analysis, the samples were cryo-milled to a fine powder using a CertiPrep 6750 freezer mill (Spex Certiprep, USA). Free lipids were removed via Soxhlet extraction for 48 h using dichloromethane:methanol (93:7; v/v). The remaining residue was air dried for 48 h and stored in a freezer at − 20 °C. Samples

Table 1
The depth, TOC (%) and organic carbon storage (Mg C ha^{-1}) for each horizon of the Wark Forest profiles.

	Depth (cm)	TOC (%)	OC (Mg C ha^{-1})
SS			
Fresh litter (L)	2.5 ± 1.1	38.1 b ± 0.26	24.7c ± 4.8
Fibric histic (Hf)	8.0 ± 4.1	42.5 a ± 1.14	30.7c ± 9.2
Mesic histic (Hm)	14.5 ± 6.0	45.5 a ± 1.31	86.5 b ± 18.9
Sapric histic (Hs)	25 ± 0.9	43.8 a ± 0.69	142.1 a ± 25.9
FM			**284.1 b**
Fresh litter (L)	2.5 ± 1.1	43.2 ± 1.27	23.8c ± 0.49
Fibric histic (Hf)	6.0 ± 1.2	40.8 ± 1.92	25.3c ± 2.44
Mesic histic (Hm)	14 ± 5.3	43.7 ± 0.87	84.7 b ± 14.18
Sapric histic (Hs)	27.5 ± 2.7	43.0 ± 0.69	163.5 a ± 18.72
OP			**297.3 b**
Fresh litter (L)	2.0 ± 0.4	40.6 b ± 1.66	14.5c ± 0.30
Fibric histic (Hf)	2.5 ± 0.1	42.7 ab ± 0.40	19.1c ± 3.66
Mesic histic (Hm)	15.0 ± 11.6	44.5 ab ± 1.52	117.0 b ± 50.46
Sapric histic (Hs)	30.5 ± 1.5	47.7 a ± 0.91	258.6 a ± 49.11
			409.2 a

from each horizon were ran in duplicate with unlabelled and ^{13}C-labelled TMAH in 2010.

2.3. THM analysis

On-line THM in the presence of unlabelled and ^{13}C-labelled TMAH was performed using a pulsed mode open pyrolysis system, specifically a CDS 1000 Pyroprobe unit (Chemical Data Systems, USA) fitted with a platinum coil and a CDS 1500 valved interface. Approximately 1 mg of extracted sample was weighed into a quartz pyrolysis tube plugged with pre-extracted silica wool. An internal standard, 5α-androstane was added to the samples to allow for accurate quantitative chromatographic analysis to be carried out on peaks within the chromatogram, and an aqueous solution of unlabelled or ^{13}C-labelled TMAH (25% w/w) was added to the sample immediately prior to THM.

In addition, a sample of living non-*Sphagnum* moss *P. commune* was analysed using unlabelled and labelled TMAH. This litter sample was sampled as part of a larger study (see Abbott et al.,[26]). This fresh sample was identified and labelled on site by Hakan Rydin (University of Uppsala, Sweden). The litter was freeze-dried and extracted as described in Section 2.2. The Pyroprobe interface was maintained at 340 °C and THM was carried out at 686 °C (actual 610 °C) for 10 s (20 °C/ms temperature ramp) with the products passing into a Hewlett-Packard 5890 gas chromatograph (GC) with an open split (40 cm^3/min) and a 60 m HP5-MS column (0.25 mm internal diameter, 0.25 μm film thickness; J&W Scientific, USA). Helium was used as carrier gas at a flow rate of 1 cm^3/min. The GC oven was programmed from 50 °C to 220 °C at a rate of 1.5 °C/min, where it was held isothermally for 1 min and then raised to a final temperature of 320 °C at a rate of 15 °C/min, where it was held for 16 min. The GC was linked to a Hewlett-Packard 5972 mass spectrometer (MS) (electron ionization voltage 70 eV, source temperature 180 °C, multiplier voltage 2000 V, interface temperature 320 °C), which was used to analyse the pyrolysis products. The data were obtained using a Hewlett-Packard Vectra 486 Chemstation computer, used in full scan mode (m/z = 50–700). Compound identification was based on the NIST98 mass spectral library, on ion fragmentation patterns and following the conventions described in other studies [39,40], together with the comparison of mass spectra and relative retention times from our previous studies [26,27]. Percentage aromatic hydroxyl content was determined using equations and mass spectral methods set out in previous work [20,41,42]. Duplicate samples of each solvent extracted soil were analysed from each horizon using both unlabelled and ^{13}C-labelled TMAH. THM in the presence of ^{13}C-TMAH was used to determine the lignin yield; lambda (Λ), correcting for any non-lignin inputs [20,43–45] together with the corrected lignin degradation proxy; the guaiacyl acid/aldehyde ratio ($[Ad/Al]_G$). The $[Ad/Al]_G$ records the state of oxidation for guaiacyl components (G6/G4) and is determined as the sum of 3,4-dimethoxybenzoic acid methyl ester (G6) divided by 3,4-dimethoxybenzaldehyde (G4) [20].

Representative partial chromatograms of the thermochemolysis products from every horizon of each peat profile are presented as Supplementary Information (Figs. S1–4).

Sphagnum acid derived products can be used to indicate the presence of *Sphagnum* spp. in the peat cores [11]. The *Sphagnum* yield (σ) was calculated according to Abbott et al., [26]. Where σ is the sum of the amounts of the four products; methylated 4-isopropenylphenol, methylated *cis* and *trans* 3-(4′hydroxyphen-1-yl)but-2-enoic acid, and methylated 3-(4′hydroxyphen-1-yl)but-3-enoic acid (I, IIa/b and III, respectively) normalised to 100 mg of organic carbon. The relative amounts of the four sphagnum acid THM products as indicators of redox conditions in young surficial peats was also established [27].

2.4. Total organic carbon, bulk density and carbon storage

Peat bulk density (D_b) was determined in duplicate for each humic horizon within each profile using 100 cm^3 soil cores. In the lab the soils were weighed, then oven dried at 60 °C for 48 h and reweighed to obtain the dry weight bulk density. The total organic carbon (TOC) content was measured in duplicate using the LECO-CS-244 analyser (Leco Corporation, USA). The organic carbon storage (Mg C/ha) in each horizon is calculated using the bulk density values, the TOC values and the horizon depths (Table 1).

The measurement of TOC content permits the normalisation of the amounts of phenols per 100 mg of organic carbon [43–45].

2.5. ^{210}Pb dating

The dried and milled peat samples were transferred into sealed polystyrene containers for ^{210}Pb analysis. The samples were left to equilibrate for at least 25 days to allow secular equilibrium to establish. The material was evenly distributed over the base of the sample cup (diameter 60 mm), thereby maximising the potential for detecting the gamma emissions from ^{210}Pb. The naturally occurring gamma ray spectrum was measured using a high purity broad energy germanium (BEGe) detector (Canberra BE3825 with a carbon epoxy window, active diameter 71 mm and active area 3100 mm^2; cryostat 7500SL-RDC-4; preamplifier 2002CSL) in the BGS Inorganic Geochemistry Laboratories. The detector was calibrated using fundamental parameters and the activities of the following radionuclides obtained: Cs 137 (661.7 keV), Pb 210 (46.5 keV), Pb 214 (351.9 keV), Bi 214 (609.3 keV) and Ra 226 (186.2 keV). The acquired spectrum was processed using proprietary Genie 2000 software (Canberra) using efficiency calibrations tailored to the geometry and density of each sample. The density of each sample was calculated from the sample geometry and the material composition used for modelling was estimated using differing proportions of peat and mineral content depending upon sample density. A user defined line library was used for peak identification and the nuclide activities have been background corrected. ^{210}Pb, a natural long-lived fallout radionuclide of the ^{238}U decay series with a half-life of 22.3 years, is a decay product of ^{226}Ra (half-life of 1622 years) and ^{222}Rn (half-life of 3.8 days) in sequence.

2.6. Statistical analysis

Statistical analysis was performed using Minitab 16 statistical software package (Minitab Inc., USA). The analysis of variance (ANOVA) was tested using the General Linear Model (GLM) method, which analyses a continuous response variable with at least one categorical factor with two or more levels to test for significant differences in the data using the p-value. Significant differences between means were evaluated at p-value of less than 0.05 (i.e. 95% confidence interval). The data residuals are required to be normally distributed with roughly equal variances between factor levels for the GLM test to be reliable. This was tested with the Anderson-Darling Normality test. The residuals are the differences between the average for the treatment and the individual observation. The p-value must be greater than 0.05 for the residuals to be considered to have a reasonably normal distribution, however the nearer to 1.0 the better. If the residuals follow a significantly different distribution to a normal one ($p < 0.05$) then the ANOVA model is not reliable. When the GLM displayed a significant difference ($p < 0.05$), and the residuals were normally distributed ($p > 0.05$), the Tukey's honestly significantly different test (HSD) was used to show significant differences, using a multiple comparison method. Data which were not normally distributed were tested for significant differences ($p < 0.05$) using the Kruskal-Wallis test. There is no Tukey's test equivalent; however a Mann-Whitney test can be used to determine pairwise differences. The standard error of the mean was calculated and displayed graphically as error bars or within the text (±).

3. Results

3.1. Aromatic THM products

THM of extracted peat soils samples yielded two sets of methylated phenolic products; vascular and non-vascular derived aromatic compounds. A list of the dominant aromatic lignin and non-lignin compounds are listed in Table 2 alongside their reference code. The full compound name and code is presented in the first instance in the main text, followed by just the codes thereafter.

The total lignin yield (Λ) across all samples was reduced by up to 50% after correction for tannin, polyhydroxy compounds, and demethylated lignin. This is a result of changes primarily to 3,4,5-trimethoxybenzoic acid methyl ester (S6), 3,4-dimethoxybenzoic acid methyl ester (G6) and ferulic acid (G18), but all lignin monomers showed that they comprise some hydroxyl species.

The first set includes the lignin derived phenols with guaiacyl (G), syringyl (S), and *p*-hydroxyphenyl (P) structures together with the methyl esters of the cinnamyl phenols, G18, and *p*-coumaric acid (P18). The addition of ^{13}C-labelled TMAH to THM allowed the distinction between lignin- and non-lignin- derived (particularly tannins) phenols and enabled each group to be analysed separately. This set included 3,4-dimethoxybenzenepropanoic acid methyl ester (G12), a marker for the non-*Sphagnum* moss *P. commune* [17]. The second set comprises four sphagnum acid pyrolysis products; methylated 4-isopropenylphenol, methylated *cis* and *trans* 3-(4′hydroxyphen-1-yl)but-2-enoic acid, and methylated 3-(4′hydroxyphen-1-yl)but-3-enoic acid (I, IIa/b and III, respectively), derived from the *Sphagnum* specific, sphagnum acid [11,26,46].

Not all THM products are observed in every trace however, and as a result, the distribution of aromatic products present can provide an indication of the vegetation inputs [15,47]. The partial chromatogram for the total ion current (TIC) of the thermochemolysis products from each horizon of each profile is presented in the Supplementary Information (Figs. S1-S4).

Table 2
The predominant aromatic compounds derived from lignins and polyphenols from the THM of the peat samples and the *m/z* of the characteristic ions. Compounds listed in order of retention time.

Reference	Compound	*m/z* (unlabelled)
P1	methoxybenzene	65, 77, 108
P2	1-methoxy-4-methylbenzene	91, 107, 122
G1	1,2-dimethoxybenzene	95, 123, 138
P3	4-methoxybenzeneethylene	91, 119, 134
G2	3,4-dimethoxytoluene	109, 137, 152
I	4-isopropenylphenol	133,148
P4	4-methoxybenzaldehyde	77, 135, 136
P5	4-methoxyacetophenone	107, 135, 150
G3	3,4-dimethoxybenzeneethylene	121, 149, 164
P6	4-methoxybenzoic acid methyl ester	77, 135, 166
P24	4-methoxybenzeneacetic acid methyl ester	91, 121, 180
G4	3,4-dimethoxybenzaldehyde	151, 165, 166
G5	3,4-dimethoxyacetophenone	137, 165, 180
G6	3,4-dimethoxybenzoic acid methyl ester	165, 181, 196
S4	3,4,5-trimethoxybenzaldehyde	125, 181, 196
IIa	(*E/Z*)- 3-(4′hydroxyphen-1-yl)-but-2-enoic acid methyl ester	175, 206
III	3-(4′hydroxyphen-1-yl)-but-3-enoic acid methyl ester	148, 206
G24	3,4-dimethoxybenzeneacetic acid methyl ester	107, 151, 210
G8	(*E*)- 1-(3,4-dimethoxyphenyl)− 2-methoxyethylene	151, 179, 194
G10	(*Z*)- 1-(3,4-dimethoxyphenyl)-methoxyprop-1-ene	165, 193, 208
P18	(*E*)- 3-(4-methoxyphenyl)− 3-propenoic acid methyl ester	133, 161, 192
S5	3,4,5-trimethoxyacetophenone	139, 195, 210
G12	3,4-dimethoxybenzenepropanoic acid methyl ester	151, 224
G11	(*E*)- 1-(3,4-dimethoxyphenyl)-methoxyprop-1-ene	165, 193, 208
IIb	(*E/Z*)- 3-(4′hydroxyphen-1-yl)-but-2-enoic acid methyl ester	175, 206
S6	3,4,5-trimethoxybenzoic acid methyl ester	195, 211, 226
S7	(*Z*)- 1-(3,4,5-trimethoxyphenyl)− 2-methoxyethylene	181, 209, 224
S8	(*E*)- 1-(3,4,5-trimethoxyphenyl)− 2-methoxyethylene	181, 209, 224
G14	*threo/erythro* 1-(3,4-dimethoxyphenyl)− 1,2,3-trimethoxypropane	166, 181, 270
G15	*threo/erythro* 1-(3,4-dimethoxyphenyl)− 1,2,3-trimethoxypropane	166, 181, 270
G18	(*E*)- 3-(3,4-dimethoxyphenyl)− 3-propenoic acid methyl ester	191, 207, 222
S14	*threo/erythro* 1-(3,4,5-trimethoxyphenyl)− 1,2,3-trimethoxybenzene	181, 211, 300
S15	*threo/erythro* 1-(3,4,5-trimethoxyphenyl)− 1,2,3-trimethoxybenzene	181, 211, 300
IS	5α-androstane	

3.2. Surface litter

The contribution of each sphagnum acid product (I, IIa/b, and III) to the total *Sphagnum* marker yield (σ) is shown in Fig. 1. The σ is greatest at the surface of the SS profiles, where all four sphagnum acid derived aromatic compounds can be seen. The four *Sphagnum* markers (I, IIa/b and III), were identified in varying quantities in the litter of the two SS profiles and the two FM profiles (Fig. 1). The SS litter (SS1 and SS2) were dominated by *Sphagnum* marker I. There were also strong inputs of *p*-hydroxyphenyl lignin units (P1, P2, P3, P6 and P18), alongside smaller inputs of G6. Small quantities of *threo/erythro* 1-(3,4,5-trimethoxyphenyl)− 1,2,3-trimethoxybenzene (S14/15), can be observed in the FM and SS litter. There is a complete absence of these intact lignin phenols in the OP (Fig. S1).

FM profile one (FM1) litter, whilst showing the presence of the four *Sphagnum* markers, is dominated by 4-methoxyacetophenone (P5); whilst the FM profile 2 (FM2) litter, is dominated by G6. The *P. commune* marker, G12 dominates the litter at the open peat profile one (OP1) (Fig. 2c). This litter was visually identified based on its physical characteristics as the non-*Sphagnum* moss, *P. commune* [48]. This methyl ester was also observed in small quantities in the litter of FM1. To confirm the presence of G12 in this plant species, a fresh plant sample of *P. commune* was sampled from Ryggmossen, Sweden. This endohydric non-*Sphagnum* moss was devoid of the four identified *Sphagnum* markers, however contained 3,4-dimethoxybenzenepropanoic acid methyl ester (*m/z* 151, 224) which dominated the trace (Fig. 3; Fig. S1). The litter of OP profile two (OP2) shows the presence of two unidentified compounds, and despite this litter appearing visually similar to *Sphagnum* moss, contains no *Sphagnum* biomarkers (Fig. S1).

Fig. 2 shows the corrected lignin (Λ) values alongside the *Sphagnum* biomarker (σ) and G12 yields, to provide an indication of the quantities of each broad vegetation group input across the site and down the cores. The FM and SS display similar quantities of aromatic lignin compound input and *Sphagnum* derived product input into the surface litter. Whilst the OP displays a dominant input of *P. commune* (Fig. 2). The lignin phenol yield of the litter is significantly lower in the OP compared to the SS ($p = 0.048$), with the FM cores demonstrating an intermediate lignin content.

3.3. Histic peat

The concentrations of *Sphagnum* markers (I, IIa/b, III) are significantly lower in the mesic and sapric peat when compared to the fresh litter and fibric peat. σ is greatest in the fibric peat of the FM and SS profiles, where all four sphagnum acid derived aromatic compounds can be seen. OP1 now indicates the presence of *Sphagnum* markers I and II, albeit in small quantities in the deeper peat (Fig. 1). Across the six profiles (OP, FM and SS), the *Sphagnum* markers IIa and III are absent from the deeper histic horizons, with I and IIb the dominant *Sphagnum* compounds down all the profile.

The SS fibric histic horizon is dominated by G6 (SS1 and SS2) and

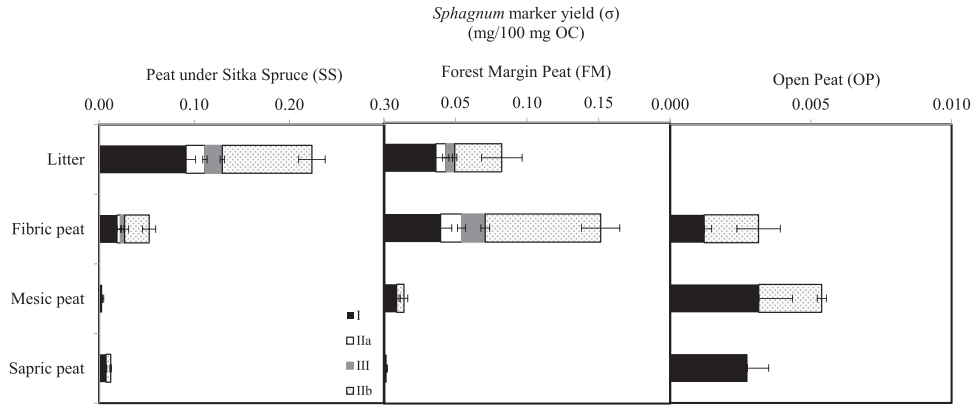

Fig. 1. Depth profiles of each sphagnum acid THM product (I; Black fill, IIa; white fill, III; grey fill, IIb: dotted fill) contributing to the *Sphagnum* (σ) yields (mg/100 mg OC) from the peat under Sitka Spruce (SS); Forest Margin Peat (FM); and the Open Peat (OP). Error bars represent the standard error of the mean for two analytical replicates for each profile.

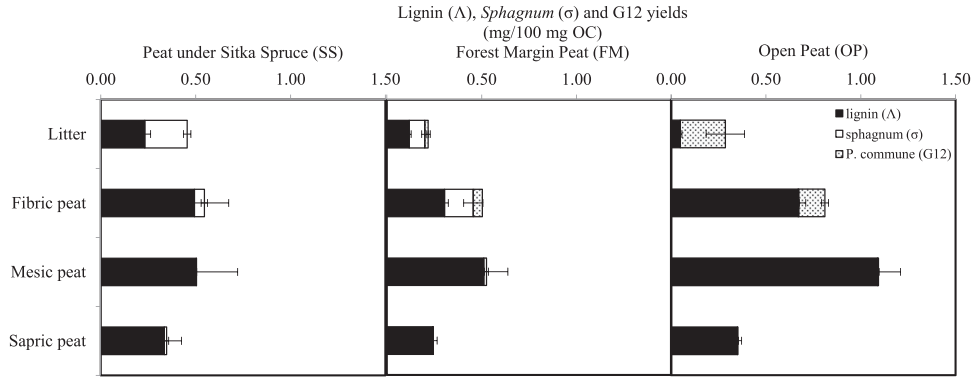

Fig. 2. Depth profiles of corrected lignin (Λ; black fill); *Sphagnum* (σ; White fill) and *P. commune* marker (G12; dotted fill) yields (mg/100 mg OC) from the peat under Sitka Spruce (SS); Forest Margin Peat (FM); and the Open Peat (OP). Error bars represent the standard error of the mean for two analytical replicates for each profile.

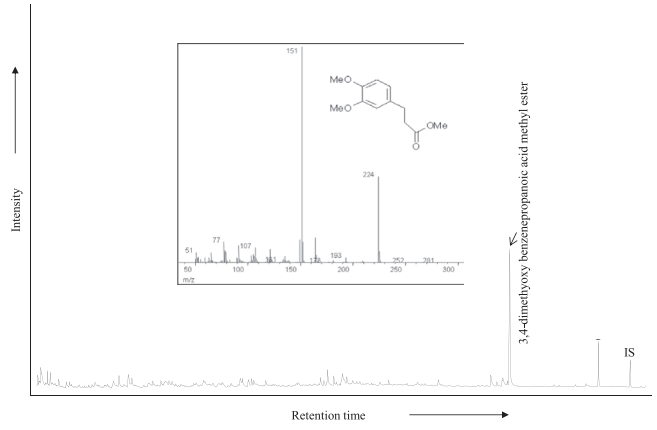

Fig. 3. The TIC of the THM products from the sample of *P. commune*. IS denotes internal standard used for quantification. Insert: The mass spectra of 3,4-dimethoxybenzenepropanoic acid methyl ester formed during TMAH treatment and the associated molecular structure.

P18 (SS1). The fibric histic horizon in FM1 shows no dominating aromatic compounds, with inputs from the four *Sphagnum* markers observed alongside P6, G4, G6 and G12; whilst FM2 is dominated by 3,4-dimethoxybenzoic acid methyl ester (G6) (Fig. S2). G12 and the two unidentified compounds remain present in high quantities in OP1 and OP2, respectively, however cinnamyl lignin phenols (*p*-coumaric acid, P18 and ferulic acid, G18) are now also dominating (Fig. 2). The fibric histic traces shown in Fig. S2, display an increased proportion of lignin phenol G6 across all the profiles.

Figs. S3 and S4 depict the THM results from the deeper, mesic histic and sapric histic horizons across all profiles. The deeper histic horizons showed no differences in the lignin yield between the profiles ($p > 0.05$). A maximum in the lignin phenols occurred in the mesic peat, which corresponds to a depth of approximately 20 cm across the site (Fig. 2). Within the deeper, mesic sapric histic peat, the *Sphagnum* and *P. commune* markers have decreased to trace levels (Fig. 2). The guaiacyl and syringyl acids (G6 and S6) and cinnamyl phenols (P18 and G18) dominate the mesic histic peat of the six profiles. G12 is not present in the deeper mesic and sapric peat (Fig. 2). Across the six profiles, the guaiacyl acid lignin phenol (G6) dominates the sapric peat. Small quantities of S14 and S15 (lignin phenols with an intact glycerol side chain) remain present at depth at the six peat cores. With the exception of the litter in OP1 and OP2, the vascular species markers dominate the aromatic content of the surficial peat cores (Fig. 2).

The acid/aldehyde ratio $[Ad/Al]_G$ is greatest at the surface of all profiles, however decreases significantly from the litter into the fibric histic horizon, below which there is a gradual increase (Fig. 4). There is an increasing proportion of I relative to the other *Sphagnum* markers in all cores with increasing depth (%σ_I; Fig. 5).

3.4. ^{210}Pb dating

^{210}Pb dating indicates the upper 50 cm of the surficial peat cores represent approximately 250–300 years of deposition (Fig. 6). Given the

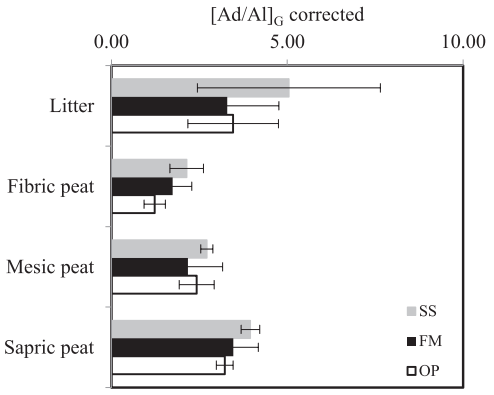

Fig. 4. Depth profiles of $[Ad/Al]_G$ ratio from the peat under Sitka Spruce pits (SS; grey fill); Forest Margin Peat pits (FM; black fill); and the Open Peat pits (OP; no fill). Error bars represent the standard error of the mean for two analytical replicates.

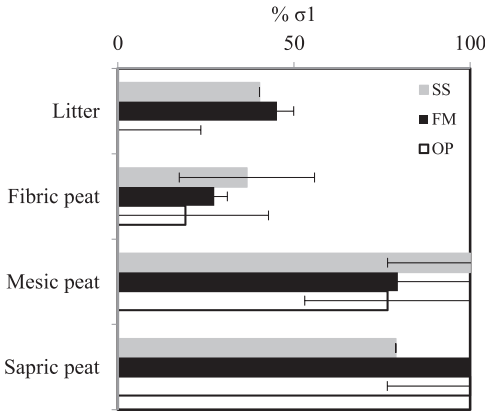

Fig. 5. Depth profiles of %σI ratio from the peat under Sitka Spruce pits (SS; grey fill); Forest Margin Peat pits (FM; black fill); and the Open Peat pits (OP; no fill). Error bars represent the standard error of the mean for two analytical replicates.

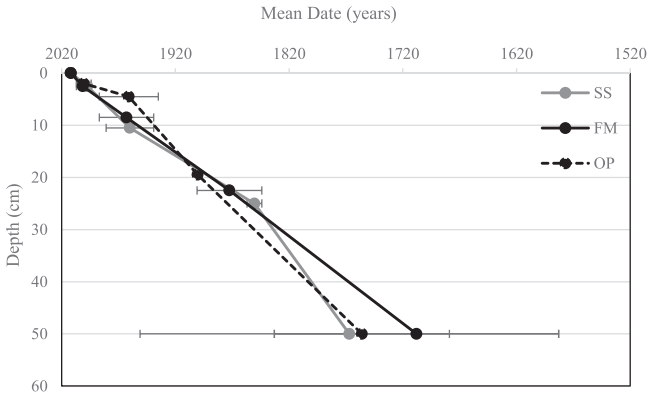

Fig. 6. ^{210}Pb dating from the peat under Sitka Spruce pits (SS; grey line); Forest Margin Peat pits (FM; black line); and the Open Peat pits (OP; dashed line). Error bars represent the standard error of the mean for two analytical replicates.

limited number of horizons sampled, the data provided an indication of the age of the peat, however has not been utilised for determining accumulation rates.

4. Discussion

4.1. Surface litter

Sphagnum acid THM products have been identified within the surficial peat cores across the three habitat areas, and serve as putative biomarkers for the contribution of *Sphagnum*-derived organic matter in organic soils, as well as providing information on peatland oxic conditions [26,27]. The occurrence of all four *Sphagnum* markers (I, IIa/b and III) in the litter of the two FM and two SS profiles reflects a current vegetation cover consisting of *Sphagnum* spp. together with vascular vegetation as indicated by the presence of lignin monomers (Fig. 2). In addition to the sphagnum acid THM products, G6 is also a dominant phenol observed in the litter of FM2. This is an indication of gymnosperm input, which are dominated by guaiacyl-based lignin (including 3, 4-dimethoxybenzoic acid methyl ester (G6)). This guaiacyl-based lignin could reflect the presence of Sitka Spruce litter at this location.

The analysis of a range of peat forming plants, including *Sphagnum*, non-*Sphagnum* and vascular species was undertaken as part of a wider study under the same conditions as those in this study [49]. *P. commune* was the only sample to contain G12 and therefore considered to serve as a biomarker for this non-*Sphagnum* moss which dominated the litter in OP1. The surface litter of OP2 has been tentatively visually identified as a common clubmoss (*Lycopodium clavatum*) [48]. This pteridophyte is distinguished apart from mosses due to the presence of a well-developed vascular system, and is often found in well drained heaths and moors, suggesting the presence of lignin phenols in this species.

Of the aromatic compounds investigated, S14/15 represent the only true lignin phenols with intact β-O-4 linkages bearing adjacent hydroxyl groups, which are derived solely from lignin [23,41]. The complete absence of these intact lignin phenols in the litter of the OP, indicates no fresh input of angiosperm vegetation to the open peat. The lower lignin phenol yield in the OP litter compared to the SS and FM litter, suggests a decrease in vascular species from the forest margin to the open peat.

The abundance of a wide range of phenols across the litter of the six profiles highlight the different surface vegetation inputs across a relatively small area. The open peat is currently colonised by primarily non-*Sphagnum* mosses, whilst the marginal peats closest to the plantation site (FM and SS profiles) display an increased species diversity, including *Sphagnum* moss, non-*Sphagnum* moss and vascular species.

4.2. Histic peat

The *Sphagnum* and *P. commune* markers decrease down the peat cores to trace levels in the mesic and sapric peat. This could be an indication of either a change in the vegetation input with time, with a reduced historic input of mosses; or the rapid loss of these diagnostic markers relative to the vascular species markers (i.e. lignin). The relative amounts of the four sphagnum acid THM products have been shown to provide an indicator of redox conditions in young surficial peats [27]. Across the profiles, I and IIb are the dominant *Sphagnum* compounds throughout the cores, however *Sphagnum* markers IIa and III are absent from the deeper histic horizons, a pattern previously observed in Swain and Abbott [27]. The increasing proportion of I relative to the other *Sphagnum* markers in all cores with increasing depth ($\%\sigma_I$; Fig. 5), supports the theory of I stabilisation with depth [27]. The consistent $\%\sigma_I$ pattern with depth for the three areas studied suggests consistent oxic conditions across the site.

Sphagnum moss is known to create conditions favourable to its growth at the expense of other vegetation [56], however, studies have shown that *Sphagnum* peatlands can become susceptible to vascular species invasion, which could reduce the carbon store capacity of the peat [57,58]. For example, a study of vegetation in an open peat area within Wark Forest between 1958 and 1986 observed an increase of grasses at the expense of *Sphagnum* spp., which was attributed to the adjacent afforested habitat altering the local hydrology [8]. Therefore,

the changes observed in this study could be due to a natural vegetation shift, or a result of changing hydrological trends (i.e. seasonal precipitation fluctuations and/or a shifting water-table due to the adjacent forest drainage (edge effect)), or impacts from climate change. These results suggest that *Sphagnum* spp. are able to survive not only perturbing environmental conditions, but are also able to establish themselves amongst non-*Sphagnum* species.

The deeper histic horizons showed no differences in the lignin yield between the six profiles suggesting a previous similar vegetation cover across the site, most likely dominated by non-woody (i.e. grassy) vascular species as indicated by the high abundance of cinnamyl phenols; P18 and G18 in the humified horizons [39,50], which is likely to be a combination of grass and heather litter input. The presence of small quantities of intact lignin phenols S14 and S15 in the deeper histic peat of all six profiles indicates an historic input of vascular, angiosperm vegetation across the site, and that despite advanced oxidation at the surface, there is no further side-chain oxidation down core.

It appears that the OP has naturally shifted from a typical heather grassland dominated by cinnamyl phenols, to a non-*Sphagnum* moss peat dominated by G12 and the potential common clubmoss marker. Whereas the FM and SS profiles have shifted from a typical heather grassland dominated by cinnamyl phenols to species-rich habitats with both *Sphagnum* spp. and vascular species present.

Across the full site, the yield of lignin phenols increased with depth from the surface litter to the fibric and mesic peat. It is unusual to see the yield of lignin phenols increase down the profile despite linearly deposited organic topsoils, however, coupled with the changes in *Sphagnum* yield (Fig. 2), this is likely reflecting a historic vegetation shift from lignin-rich vascular species to non-vascular species (i.e. *Sphagnum* and non-*Sphagnum* mosses), reducing the input of lignin phenols to the upper litter horizons across the site.

Across the six profiles, the $[Ad/Al]_G$ decreases into the fibric histic horizon, followed by a gradual increase (Fig. 4), indicating the progressive oxidation of lignin with increasing depth which is consistent across the site [53,54]. The results support the theory proposed by Schellekens et al. [55] of lignin decay as a surface process. It must be noted that a Cannizzaro type reaction might affect the THM method, in which a disproportionation of the aldehyde occurs, resulting in production of the corresponding methoxybenzoic acid methyl ester and methoxybenzyl alcohol methyl ether [51,52]. This could particularly affect the lignin proxies that incorporate methoxybenzoic acid methyl esters, such as the acid/ aldehyde ratios, indicating the relative state of lignin oxidation. The consistent $[Ad/Al]_G$ pattern with depth suggests consistent vascular degradation. Coupled with the consistent $\%\sigma_I$ pattern with depth, suggests consistent oxic conditions across the site. Further suggesting that the changes in aromatic compounds within the surficial peat reflect a historic change in the vegetation input.

4.3. ^{210}Pb dating

^{210}Pb which occurs in situ from ^{226}Ra decay in soil and rock, is designated as "supported" ^{210}Pb decay while ^{210}Pb from atmospheric ^{222}Rn decay, which in turn occurs from ^{226}Ra decay in soil and rock, is designated as "unsupported" ^{210}Pb decay. The deposition of fallout ^{210}Pb from the atmosphere has been relatively constant over time because of its natural origin. The supported ^{210}Pb activity has been calculated from the average of the activities of ^{214}Pb (t½ 29.6 min) and ^{214}Bi (t½ 19.8 min) where possible, for particularly light or low density samples or where the uncertainty on the less sensitive ^{214}Bi peak was too great, the activity of only ^{214}Pb was used to estimate the supported ^{210}Pb activity. The unsupported ^{210}Pb activity is calculated by difference between the measured activity and the supported ^{210}Pb activity. The activity of ^{137}Cs (t½ 30.05 y) is also monitored to provide a level of data validation assuming the activity is a result from the atomic weapons testing which reached a peak of in 1963 just before the nuclear test ban treaty or from the Chernobyl reactor incident in 1986. If measurable, the activity of ^{226}Ra is used for comparison only as the spectral peak suffers from interference from ^{235}U. The most common ^{210}Pb dating models are the constant activity model (CA, also known as constant initial concentration, CIC) [59], the constant flux and constant sedimentation rate model (CFCS) [60,61] and the constant flux model (CF, also called constant rate of supply, CRS) [62]. In those models, unsupported ^{210}Pb was assumed to be immobile once deposited and not migrated downwards to the sediment column.

The maximum of lignin products found at around 20 cm across all six profiles can be attributed to a change in the dominant vegetation cover between approximately 1900 and 1960 across the site (Fig. 6). This coincides with the planting date of the adjacent plantation and thus the vegetation shift of the unplanted heath grassland coincides with adjacent site disturbance and associated changes in the soil properties.

5. Conclusions

Aromatic biomacromolecules from the upper 50 cm of cambic stagnohumic gley soil were characterised by ^{13}C TMAH thermochemolysis across marginal peat between a Sitka spruce plantation and open peat to explore the range of semi-natural vegetation establishing across this habitat following adjacent forestry planting on these peaty soils. Distinct aromatic compounds from *Sphagnum* mosses, non-*Sphagnum* mosses and vascular plants were identified in one analysis, illustrating a shift in the vegetation from a historic grass-dominated vegetation across the site, to a current mixed vegetation cover of vascular plants, *Sphagnum* spp. and non-*Sphagnum* mosses, which vary in distribution across the site. The surficial peat was dated using ^{210}Pb, indicating a vegetation shift between approximately 1900 and 1960, where a maximum of vascular plant inputs was observed across the full site, which corresponds with the planting date of the adjacent plantation.

Further work could utilise this rapid screening method coupled with detailed carbon analysis of the peat core and ^{210}Pb dating to investigate the change in vegetation over time and how it relates to peat- and carbon accumulation.

Declaration of Competing Interest

The authors declare that they have no known competing financial interests or personal relationships that could have appeared to influence the work reported in this paper.

Data Availability

Data will be made available on request.

Acknowledgements

The authors wish to thank Prof. Håkan Rydin (University of Uppsala, Sweden) for identifying the *P. commune* plant samples which were collected as part of a Natural Environment Research Council Project (NERC grant: NE/E004938/1); Christopher Vane (BGS) for the ^{210}Pb dating of the peat samples; and Dr. Timothy Filley for the generous gift of ^{13}C-TMAH. We also thank NERC and Forest Research for a research studentship to EYR. The authors would also wish to thank three anonymous reviewers for their constructive comments which improved this manuscript.

Appendix A. Supporting information

Supplementary data associated with this article can be found in the online version at doi:10.1016/j.jaap.2023.106008.

References

[1] Z. Yu, J. Loisel, D.P. Brosseau, D.W. Beilman, S.J. Hunt, Global peatland dynamics since the Last Glacial Maximum, Geophys. Res. Lett. 37 (2010) L13402, https://doi.org/10.1029/2010GL043584.

[2] O.M. Bragg, Hydrology of peat-forming wetlands in Scotland, Sci. Total Environ. 294 (2002) 111–129, https://doi.org/10.1016/S0048-9697(02)00059-1.

[3] M.G.R. Cannell, R.C. Dewar, D.G. Pyatt, Conifer plantations on drained peatlands in Britain: a net gain or loss of carbon? Forestry 66 (1993) 353–369, https://doi.org/10.1093/forestry/66.4.353.

[4] H. Tiessen, J.W.B. Stewart, Particle-size fractions and their use in studies of soil organic matter: II. Cultivation effects on organic matter composition in size fractions, Soil Sci. Soc. Am. J. 47 (1983) 509–514, https://doi.org/10.2136/sssaj1983.03615995004700030023x.

[5] G.R. Hillman, Some hydrological effects of peatland drainage in Alberta's boreal forest, Can. J. . Res 22 (1992) 1588–1596, https://doi.org/10.1139/x87-019.

[6] W. Mojeremane, R.M. Rees, M. Mencuccini, Effects of site preparation for afforestation on methane fluxes at Harwood Forest, NE England, Biogeochemistry 97 (2010) 89–107. https://www.jstor.org/stable/25652621.

[7] M. Robinson, R.E. Moore, T.R. Nisbet, J.R. Blackie, From moorland to forest: the Coalburn catchment experiment. Wallingford, Inst. Hydrol. (IH Report no.133) (1998) 72. http://nora.nerc.ac.uk/7372/1/IH_133.pdf.

[8] S.B. Chapman, R.J. Rose, Changes in the vegetation at Coom Rigg Moss National Nature Reserve within the period 1958-86, J. Appl. Ecol. 28 (1991) 140–153, https://doi.org/10.2307/2404121.

[9] R. Farmer, Active blanket bogs in Wales, EU LIFE (2011) 58.

[10] H. Rudolph, J. Samland, Occurrence and metabolism of sphagnum acid in the cell walls of bryophytes, Phytochemistry 24 (1985) 745–749, https://doi.org/10.1016/S0031-9422(00)84888-8.

[11] E. van der Heijden, A combined anatomical and pyrolysis mass spectrometric study of peatified plant tissues, PhD Thesis Univ. Van. Amst., Amst. (1994).

[12] R.L. Crawford, Lignin Biodegradation and Transformation, Wiley, New York, 1981.

[13] M.H. Gold, H. Wariishi, K. Valli, Extracellular peroxidases involved in lignin degradation by the white rot basidiomycete *Phanerochate chrysosporium*, ACS Symp. . Ser. 389 (1989) 127–140, https://doi.org/10.1021/bk-1989-0389.ch009.

[14] W. Boerjan, J. Ralph, M. Baucher, Lignin biosynthesis, Annu. Rev. Plant Biol. 54 (2003) 519–546, https://doi.org/10.1146/annurev.arplant.54.031902.134938.

[15] T. Higuchi, Lignin structure and morphological distribution in plant cell walls, in: T.K. Kirk, T. Higuchi, H.-m. Chang (Eds.), Lignin Biodegradation: Microbiology, 1980, Chemistry, and Potential Applications, CRC Press, Florida, 1980, pp. 1–20.

[16] UK Centre for Ecology and Hydrology (UKCEH) Countryside Survey UKCEH Countryside Survey | UK-SCAPE | UK Centre for Ecology & Hydrology 2007 (Accessed 28 February 2023).

[17] K.G.J. Nierop, G.J.M. Versteegh, T.R. Filley, J.W. de Leeuw, Quantitative analysis of diverse sporomorph-derived sporopollenins, Phytochemistry 162 (2019) 207–215, https://doi.org/10.1016/j.phytochem.2019.03.023.

[18] T.R. Filley, P.G. Hatcher, W.C. Shortle, R.T. Praseuth, The application of ^{13}C-labeled tetramethylammonium hydroxide (^{13}C-TMAH) thermochemolysis to the study of fungal degradation of wood, Org. Geochem. 31 (2000) 181–198, https://doi.org/10.1016/S0146-6380(99)00159-X.

[19] T.R. Filley, G.D. Cody, B. Goodell, J. Jellison, C. Noser, A. Ostrofsky, Lignin demethylation and polysaccharide decomposition in spruce sapwood degraded by brown rot fungi, Org. Geochem. 33 (2002) 111–124, https://doi.org/10.1016/S0146-6380(01)00144-9.

[20] T.R. Filley, K.G.J. Nierop, Y. Wang, The contribution of polyhydroxyl aromatic compounds to tetramethylammonium hydroxide lignin-based proxies, Org. Geochem. 37 (2006) 711–727, https://doi.org/10.1016/j.orggeochem.2006.01.005.

[21] S.W. Frazier, L.A. Kaplan, P.G. Hatcher, Molecular characterization of biodegradable dissolved organic matter using bioreactors and [^{12}C/^{13}C] tetramethylammonium hydroxide thermochemolysis GC-MS, Environ. Sci. Technol. 39 (2005) 1479–1491, https://doi.org/10.1021/es0494959.

[22] S.L. Mason, T.R. Filley, G.D. Abbott, A comparative study of the molecular composition of a grassland soil with adjacent unforested and afforested moorland ecosystems, Org. Geochem. 42 (2012) 1519–1528, https://doi.org/10.1016/j.orggeochem.2010.11.003.

[23] K.G.J. Nierop, T.R. Filley, Assessment of lignin and (poly-)phenol transformations in oak (*Quercus robur*) dominated soils by ^{13}C-TMAH thermochemolysis, Org. Geochem. 38 (2007) 551–565, https://doi.org/10.1016/j.orggeochem.2006.12.007.

[24] C. Saiz-Jimenez, Analytical pyrolysis of humic substances: Pitfalls, limitations, and possible solutions, Environ. Sci. Technol. 28 (1994) 1773–1780, https://doi.org/10.1021/es00060a005.

[25] J.M. Challinor, A pyrolysis-derivatisation-gas chromatography technique for the structural elucidation of some synthetic polymers, J. Anal. Appl. Pyrolysis 16 (1989) 323–333, https://doi.org/10.1016/0165-2370(89)80015-4.

[26] G.D. Abbott, E.Y. Swain, A.B. Muhammad, K. Allton, L.R. Belyea, C.G. Laing, G. L. Cowie, Effect of water-table fluctuations on the degradation of *Sphagnum* phenols in surficial peats, Geochim. Cosmochim. Acta 106 (2013) 177–191, https://doi.org/10.1016/j.gca.2012.12.013.

[27] E.Y. Swain, G.D. Abbott, The effect of redox conditions on sphagnum acid thermochemolysis product distributions in a northern peatland, J. Anal. Appl. Pyrolysis (2013) 2–7, https://doi.org/10.1016/j.jaap.2012.12.022.

[28] J.C. Coulson, J. Butterfield, An investigation of the biotic factors determining the rates of plant decomposition on blanket bog, J. Ecol. (1978) 631–650, https://doi.org/10.2307/2259155.

[29] E. van der Heijden, J.J. Boon, S. Rasmussen, H. Rudolph, Sphagnum acid and its decarboxylation product isopropenylphenol as biomarkers for fossilised sphagnum in peats, Anc. Biomol. (1997) 93–107.

[30] L.C. Johnson, A.W.H. Damman, Species-controlled sphagnum decay on a south Swedish raised bog, Oikos 61 (1991) 234–242, https://doi.org/10.2307/3545341.

[31] M.R. Turetsky, S.E. Crow, R.J. Evans, D.H. Vitt, R.K. Wieder, Trade-offs in resource allocation among moss species control decomposition in boreal peatlands, J. Ecol. 96 (2008) 1297–1305, https://doi.org/10.1111/j.1365-2745.2008.01438.x.

[32] D. Yeloff, D. Mauquoy, The influence of vegetation composition on peat humification: implications for palaeoclimatic studies, Boreas 35 (2006) 662–673, https://doi.org/10.1111/j.1502-3885.2006.tb01172.x.

[33] M. Turetsky, S.W. Manning, R.K. Wieder, Dating recent peat deposits, Wetlands 24 (2004) 324–356, https://doi.org/10.1672/0277-5212(2004)024[0324:DRPD]2.0.CO;2.

[34] A. Cwanek, E. Łokas, E.A.D. Mitchell, Y. Mazei, P. Gaca, J.A. Milton, Temporal variability of Pu signatures in a ^{210}Pb-dated *Sphagnum* peat profile from the Northern Ural, Russian Federation, Chemosphere 281 (2021), 130962, https://doi.org/10.1016/j.chemosphere.2021.130962.

[35] G.F. Peterken, D. Ausherman, M. Buchenau, R.T.T. Forman, Old-growth conservation within British upland conifer plantations, Forestry 65 (1992) 127–144, https://doi.org/10.1093/forestry/65.2.127.

[36] NERC (CEH), 2017 Land cover map 2015 Land Cover Map 2015 - EIDC (ceh.ac.uk) https://catalogue.ceh.ac.uk/documents/0255c014–1630-4c2f-bc05–48a6400dd045 (Accessed 28 February 2023).

[37] B.W. Avery, Soil Classification for England and Wales, in: Technical monograph (Soil Survey of England and Wales), no. 14, Harpenden,, 1980, p. 67.

[38] FAO, 2011 5. CLASSIFICATION (fao.org) https://www.fao.org/3/x5872e/x5872e07.htm (Accessed 28 February 2023).

[39] D.J. Clifford, D.M. Carson, D.E. McKinney, J.M. Bortiatynski, P.G. Hatcher, A new rapid technique for the characterization of lignin in vascular plants: thermochemolysis with tetramethylammonium hydroxide (TMAH), Org. Geochem. 23 (1995) 169–175, https://doi.org/10.1016/0146-6380(94)00109-E.

[40] P.G. Hatcher, M.A. Nanny, R.D. Minard, S.D. Dible, D.M. Carson, Comparison of two thermochemolytic methods for the analysis of lignin in decomposing gymnosperm wood: the CuO oxidation method and the method of thermochemolysis with tetramethylammonium hydroxide (TMAH), Org. Geochem. 23 (1995) 88–888, https://doi.org/10.1016/0146-6380(95)00087-9.

[41] T.R. Filley, R.D. Minard, P.G. Hatcher, Tetramethylammonium hydroxide (TMAH) thermochemolysis: proposed mechanisms based upon the application of ^{13}C-labeled TMAH to a synthetic model lignin dimer, Org. Geochem. 30 (1999) 607–621, https://doi.org/10.1016/S0146-6380(99)00040-6.

[42] S.L. Mason, T.R. Filley, G.D. Abbott, The effect of afforestation on the soil organic carbon (SOC) of a peaty gley soil using on-line thermally assisted hydrolysis and methylation (THM) in the presence of ^{13}C-labelled tetramethylammonium hydroxide (TMAH), J. Anal. Appl. Pyrolysis 85 (2009) 417–425, https://doi.org/10.1016/j.jaap.2008.11.005.

[43] J.I. Hedges, D.C. Mann, The characterization of plant tissues by their lignin oxidation products, Geochim. Cosmochim. Acta 43 (1979) 1803–1807, https://doi.org/10.1016/0016-7037(79)90028-0.

[44] J.I. Hedges, J.R. Ertel, E.B. Leopold, Lignin geochemistry of a Late Quaternary sediment core from Lake Washington, Geochim. Cosmochim. Acta 46 (1982) 1869–1877, https://doi.org/10.1016/0016-7037(82)90125-9.

[45] I. Kögel, Estimation and decomposition pattern of the lignin component in forest humus layers, Soil Biol. Biochem. 18 (1986) 589–594, https://doi.org/10.1016/0038-0717(86)90080-5.

[46] E. van der Heijden, J.J. Boon, S. Rasmussen, H. Rudolph, Sphagnum acid and its decarboxylation product isopropenylphenol as biomarkers for fossilised sphagnum in peats, Anc. Biomol. 1 (1997) 93–107.

[47] K.G.J. Nierop, C.M. Preston, J. Kaal, Thermally assisted hydrolysis and methylation of purified tannins from plants, Anal. Chem. 77 (2005) 5604–5614, https://doi.org/10.1021/ac050564r.

[48] P. Taylor, British Ferns and Mosses, The Chiswick Press, London, 1960, p. 231.

[49] E.Y. Swain, Molecular characterization of terrestrial organic carbon in some organic-rich soils in the northern latitudes, PhD Thesis, Newctle. Univ. 273 (2013).

[50] J.I. Hedges, D.C. Mann, The lignin geochemistry of marine sediments from the southern Washington coast, Geochim. Cosmochim. Acta 43 (1979) 1809–1818, https://doi.org/10.1016/0016-7037(79)90029-2.

[51] P.G. Hatcher, R.D. Minard, Comment on the origin of benzenecarboxylic acids in pyrolysis methylation studies, Org. Geochem. 23 (1995) 991–994, https://doi.org/10.1016/0146-6380(95)00071-2.

[52] I. Tanczos, K. Rendl, H. Schmidt, The behavior of aldehydes—produced as primary pyrolysis products—in the thermochemolysis with tetramethylammonium hydroxide, J. Anal. Appl. Pyrolysis 49 (1999) 319–327, https://doi.org/10.1016/S0165-2370(98)00132-6.

[53] Y. Huang, G. Eglinton, E.R.E. Van Der Hage, J.J. Boon, R. Bol, P. Ineson, Dissolved organic matter and its parent organic matter in grass upland soil horizons studied by analytical pyrolysis techniques, Eur. J. Soil Sci. 49 (1998) 1–15.

[54] C.H. Vane, S.C. Martin, C.E. Snape, G.D. Abbott, Degradation of lignin in wheat straw during growth of the oyster mushroom (*Pleurotus ostreatus*) using off-line thermochemolysis with tetramethylammonium hydroxide and solid-state 13C NMR. J, Agric. Food Chem. 49 (2001) 2709–2716, https://doi.org/10.1021/JF001409A.

[55] J. Schellekens, P. Buurman, T.W. Kuyper, G.D. Abbott, X. Pontevedra-Pombal, A. Martínez-Cortizas, Influence of source vegetation and redox conditions on lignin-based decomposition proxies in graminoid-dominated ombrotrophic peat

(Penido Vello, NW Spain), Geoderma 237– 238 (2015) 270–282, https://doi.org/10.1016/j.geoderma.2014.09.012.
[56] N. van Breemen, How *Sphagnum* bogs down other plants, Trends Ecol. Evol. 10 (1995) 270–275, https://doi.org/10.1016/0169-5347(95)90007-1.
[57] H.B.M. Tomassen, A.J.P. Smolders, L.P.M. Lamers, J.G.M. Roelofs, Stimulated growth of *Betula pubescens* and *Molinia caerulea* on ombrotrophic bogs: Role of high levels of atmospheric nitrogen deposition, J. Ecol. 91 (2003) 357–370, https://doi.org/10.1046/j.1365-2745.2003.00771.x.
[58] H.B.M. Tomassen, A.J.P. Smolders, J. Limpens, L.P.M. Lamers, J.G.M. Roelofs, Expansion of invasive species on ombrotrophic bogs: Desiccation, Or. High. N. Depos. ? J. Appl. Ecol. 41 (2004) 139–150, https://doi.org/10.1111/j.1365-2664.2004.00870.x.
[59] P.G. Appleby, F. Oldfield, R.N. Thompson, P. Huttunen, K.E. Tolonen, ^{210}Pb dating of annually laminated lake sediments from Finland, Nature 280 (1979) 53–55, https://doi.org/10.1038/280053a0.
[60] P.G. Appleby, F. Oldfield, The calculation of lead-210 dates assuming a constant rate of supply of unsupported lead-210 to the sediment, Catena 5 (1978) 1–8, https://doi.org/10.1016/S0341-8162(78)80002-2.
[61] P.G. Appleby, F. Oldfield, in: M. Ivanovich, R.S. Harman (Eds.), Application of lead-210 to sedimentation studies. In Uranium-series disequilibrium: applications to earth, marine, and environmental science, Oxford University Press, 1992.
[62] J.A. Robbins, D.N. Edgington, Determination of recent sedimentation rates in Lake Michigan using Pb-210 and Cs-137, Geochim. Cosmochim. Acta 39 (1975) 285–304.